

Article

Genome-Wide Analysis and Expression of *Cyclic Nucleotide-Gated Ion Channel (CNGC)* Family Genes under Cold Stress in Mango (*Mangifera indica*)

Yajie Zhang ^{1,†}, Yubo Li ^{2,3,†}, Jing Yang ¹, Xinli Yang ⁴, Shengbei Chen ⁵, Zhouli Xie ⁶, Mingjie Zhang ¹, Yanlei Huang ⁷, Jinghong Zhang ^{1,8,*} and Xing Huang ^{2,9,10,*} 

¹ Hainan Climate Center, Haikou 570203, China

² Environment and Plant Protection Institute, Chinese Academy of Tropical Agricultural Sciences, Haikou 571101, China

³ College of Tropical Crops, Hainan University, Haikou 570228, China

⁴ Guilinyang Campus, Qiongtai Normal University, Haikou 571127, China

⁵ Hainan Meteorological Service Center, Haikou 570203, China

⁶ School of Life Sciences, Peking University, Beijing 100871, China

⁷ College of Plant Science and Technology, Huazhong Agricultural University, Wuhan 430070, China

⁸ Key Laboratory of South China Sea Meteorological Disaster Prevention and Mitigation of Hainan Province, Haikou 570203, China

⁹ Key Laboratory of Integrated Pest Management on Tropical Crops, Ministry of Agriculture and Rural Affairs, Haikou 571101, China

¹⁰ Hainan Key Laboratory for Monitoring and Control of Tropical Agricultural Pests, Haikou 571101, China

* Correspondence: janezhjh@163.com (J.Z.); hxalong@gmail.com (X.H.)

† These authors contributed equally to this work.



Citation: Zhang, Y.; Li, Y.; Yang, J.; Yang, X.; Chen, S.; Xie, Z.; Zhang, M.; Huang, Y.; Zhang, J.; Huang, X. Genome-Wide Analysis and Expression of *Cyclic Nucleotide-Gated Ion Channel (CNGC)* Family Genes under Cold Stress in Mango (*Mangifera indica*). *Plants* **2023**, *12*, 592. <https://doi.org/10.3390/plants12030592>

Academic Editors: Sylvie Renault and Janusz J. Zwiazek

Received: 28 November 2022

Revised: 15 January 2023

Accepted: 20 January 2023

Published: 29 January 2023



Copyright: © 2023 by the authors. Licensee MDPI, Basel, Switzerland. This article is an open access article distributed under the terms and conditions of the Creative Commons Attribution (CC BY) license (<https://creativecommons.org/licenses/by/4.0/>).

Abstract: The ‘king of fruits’ mango (*Mangifera indica*) is widely cultivated in tropical areas and has been threatened by frequent extreme cold weather. *Cyclic nucleotide-gated ion channel (CNGC)* genes have an important function in the calcium-mediated development and cold response of plants. However, few *CNGC*-related studies are reported in mango, regardless of the mango cold stress response. In this study, we identified 43 *CNGC* genes in mango showing tissue-specific expression patterns. Five *MiCNGCs* display more than 3-fold gene expression induction in the fruit peel and leaf under cold stress. Among these, *MiCNGC9* and *MiCNGC13* are significantly upregulated below 6 °C, suggesting their candidate functions under cold stress. Furthermore, cell membrane integrity was damaged at 2 °C in the mango leaf, as shown by the content of malondialdehyde (MDA), and eight *MiCNGCs* are positively correlated with MDA contents. The high correlation between *MiCNGCs* and MDA implies *MiCNGCs* might regulate cell membrane integrity by regulating MDA content. Together, these findings provide a valuable guideline for the functional characterization of *CNGC* genes and will benefit future studies related to cold stress and calcium transport in mango.

Keywords: mango; *CNGC*; phylogeny; cold stress; expression; malondialdehyde

1. Introduction

The *cyclic nucleotide-gated ion channel (CNGC)* family belongs to nonselective cation channels, which enable the uptake of ions, including K⁺, Ca²⁺ and Na⁺ [1]. The channel gate-control function of *CNGC* genes confers their essential roles in regulating plant growth and development [2]. Furthermore, members of the *CNGC* family are reported to mediate cellular ion homeostasis to regulate abiotic and biotic stress response [3]. Usually, plant *CNGC* genes contain six transmembrane domains, in which the cyclic nucleotide-binding domain (CNBD) is between the fifth and sixth transmembrane domains [4]. The CNBD domain is highly conserved and could be used to identify *CNGC* genes among plant species [5]. To date, the *CNGC* family has been widely reported in many plant species,

such as in *Arabidopsis thaliana* (20), *Atalantia buxifolia* (31), *Brassica oleracea* (26), *Brassica rapa* (29), *Citrus grandis* (30), *Citrus reticulata* (27), *Citrus sinensis* (32), *Gossypium hirsutum* (40), *Gossypium barbadense* (41), *Gossypium herbaceum* (20), *Gossypium arboreum* (20), *Gossypium raimondii* (20), *Nicotiana tabacum* (35), *Oryza sativa* (16), *Poncirus trifoliata* (30), *Pyrus bretschneideri* (21), *Solanum tuberosum* (20), *Triticum aestivum* (47), *Zea mays* (12) and *Ziziphus jujuba* (15) [2,5–7]. Most importantly, their functions have been well characterized in model plant *Arabidopsis*. For example, 15 *AtCNGCs* (*AtCNGC1-10/12/14/16/18/20*) are encoded Ca^{2+} -permeable channels [8], and numerous studies confirm their functions in plant development, such as *AtCNGC2* in leaf senescence, *AtCNGC3* in germination, *AtCNGC5/6/9* in root hair development, *AtCNGC7/8* in male fertility, *AtCNGC14* in root gravitropism and *AtCNGC16/18* in pollen development [9–15]. Several *AtCNGCs* are involved in stress response, including *AtCNGC1/10/19/20* in salt stress, *AtCNGC2/4/11/12* in abiotic stress, *AtCNGC2/5/6/9/12* in stomatal defense and *AtCNGC6* in heat stress [16–22]. Together, these findings provide valuable references for functional characterization and application of CNGC genes in non-model plant species.

Mango, known as the ‘king of fruits’, is one of the most popular fruits [23]. Its annual fruit yield ranks fifth around the world [24]. The main cultivated *Mangifera* species in the tropical areas around the world is *Mangifera indica* [25]. As a typical tropical plant, mango is sensitive to cold temperature [26], especially frequent extreme cold weather, which has significantly threatened to mango production in recent years [27]. However, few studies have revealed the molecular basis of cold stress response in mango trees, even if the cold storage of detached fruits has been well studied [28]. Considering that overexpression of CNGC genes promotes rice cold tolerance, we conducted genome-wide analysis of the CNGC family in mango and evaluated its expression in mango tissues, as well as that under cold stress [29]. The results showed that expression of several *MiCNGCs* was upregulated under cold temperature and highly correlated to leaf damage index malondialdehyde (MDA) contents, implying their beneficial roles in regulating mango cold tolerance. Therefore, our study will offer guidance for functional characterization of CNGC genes and benefit future studies in mango.

2. Results

2.1. Characterisation of CNGC Family in Mango

The *Arabidopsis* and rice CNGC genes were selected to search homologous genes in the genomes of *Amborella trichopoda*, sweet orange (*Citrus sinensis*) and mango [24,30,31]. Because sweet orange belongs to the Sapindales order together with mango, it was selected as a nearby reference [24]. *Amborella* was chosen as the outgroup reference to the Sapindales order since it is the basal angiosperm [30]. As a result, 7, 33 and 43 CNGC genes were identified in above three species (Tables 1 and S1). In mango species, these genes ranged from 399 to 2343 bp with predicted protein lengths of 132–780 aa. Their molecular weights and theoretical pI ranged from 14907.27 to 89883.31 Da and 4.88 to 9.67, respectively. Most of them (36 of 43) were predicted to be located at the plasma membrane, contain 3–7 transmembrane helices (Figure S1). Five and two were predicted to be nuclear and extracellular, respectively. There was no more than one transmembrane helix in these seven genes. A total of 39 mango CNGC genes were distributed at 13 chromosomes. Two major gene clusters, including 10 and 12 CNGC genes at chromosomes 9 and 15, respectively, were labeled (Figure 1).

Table 1. Characterization of mango CNGC genes, including their accession numbers, chromosome positions, the lengths of coding sequences and predicted proteins, pI and subcellular locations.

Gene ID	Accession Number	Chromosome Position	Coding Sequence (bp)	Predicted Protein (aa)	Molecular Weight (Da)	Theoretical pI	Subcellular Localization
MiCNGC1	LOC123217317	Chr1: 26617757–26622513 (+)	2088	695	80,238.87	8.59	Plasma Membrane (4.159)
MiCNGC2	LOC123202006	Chr2: 18877379–18881267 (–)	2115	704	80,732.55	9.33	Plasma Membrane (4.168)
MiCNGC3	LOC123211819	Chr3: 6181866–6187338 (+)	2298	765	88,428.88	9.17	Plasma Membrane (3.621)
MiCNGC4	LOC123223438	Chr8: 1942929–1947032 (+)	2151	716	82,987.45	9.38	Plasma Membrane (3.546)
MiCNGC5	LOC123224898	Chr9: 570085–574702 (–)	1734	577	67,095.52	9.67	Plasma Membrane (3.860)
MiCNGC6	LOC123225620	Chr9: 590058–593780 (–)	1203	400	46,407.24	9.12	Plasma Membrane (2.575)
MiCNGC7	LOC123225300	Chr9: 599306–603542 (+)	1998	665	77,653.8	9.42	Plasma Membrane (3.398)
MiCNGC8	LOC123225621	Chr9: 608291–611565 (+)	1377	458	53,035.69	9.52	Plasma Membrane (2.835)
MiCNGC9	LOC123225476	Chr9: 613450–633947 (–)	1821	606	69,498.22	5.61	Plasma Membrane (3.921)
MiCNGC10	LOC123225622	Chr9: 613655–614273 (+)	516	171	19,510.66	4.88	Nuclear (2.027)
MiCNGC11	LOC123225623	Chr9: 640657–644088 (–)	1260	419	48,200.04	5.71	Plasma Membrane (2.541)
MiCNGC12	LOC123226204	Chr9: 654424–660087 (–)	1731	576	66,396.96	8.51	Plasma Membrane (3.243)
MiCNGC13	LOC123225899	Chr9: 662666–667252 (–)	2130	709	81,778.71	9.18	Plasma Membrane (4.474)
MiCNGC14	LOC123224819	Chr9: 17603913–17607726 (–)	2151	716	82,061.84	9.54	Plasma Membrane (4.714)
MiCNGC15	LOC123226709	Chr10: 13110947–13113872 (+)	1023	340	38,771.01	9.24	Plasma Membrane (2.866)
MiCNGC16	LOC123193626	Chr12: 337616–340675 (–)	1635	544	61,685.37	8.3	Plasma Membrane (3.945)
MiCNGC17	LOC123195239	Chr13: 132576–141356 (+)	2208	735	83,845.52	9.06	Plasma Membrane (4.347)
MiCNGC18	LOC123195166	Chr13: 2244118–2249930 (+)	2193	730	84,150.34	8.66	Plasma Membrane (4.075)
MiCNGC19	LOC123196387	Chr14: 571224–582588 (–)	2343	780	89,883.31	9.05	Plasma Membrane (4.810)
MiCNGC20	LOC123196103	Chr14: 2913165–2916467 (+)	2148	715	82,156.57	8.92	Plasma Membrane (4.612)
MiCNGC21	LOC123198417	Chr15: 882187–884231 (+)	729	242	28,545.32	9.19	Nuclear (1.618)
MiCNGC22	LOC123198080	Chr15: 884570–888789 (+)	1716	571	66,348.13	6.17	Plasma Membrane (3.842)
MiCNGC23	LOC123198017	Chr15: 894806–897058 (+)	1266	421	48,693.95	5.97	Plasma Membrane (4.227)
MiCNGC24	LOC123197882	Chr15: 899688–903479 (+)	1809	602	70,104.71	8.73	Plasma Membrane (4.512)
MiCNGC25	LOC123198019	Chr15: 937711–939887 (–)	744	247	28,653.79	8.06	Nuclear (1.582)
MiCNGC26	LOC123198301	Chr15: 944971–947978 (–)	1563	520	59,757.67	8.86	Plasma Membrane (3.850)
MiCNGC27	LOC123197889	Chr15: 957259–959253 (–)	708	235	27,110.7	9.57	Extracellular (1.327)
MiCNGC28	LOC123197890	Chr15: 968337–969069 (–)	399	132	14,907.27	8.37	Extracellular (1.999)
MiCNGC29	LOC123197893	Chr15: 998581–1002107 (–)	1524	507	58,308.01	8.81	Plasma Membrane (4.361)
MiCNGC30	LOC123197894	Chr15: 1002388–1013277 (–)	1926	641	74,391.25	8.83	Plasma Membrane (4.326)
MiCNGC31	LOC123198006	Chr15: 1014910–1019679 (–)	2130	709	81,816.51	9.13	Plasma Membrane (4.548)
MiCNGC32	LOC123197621	Chr15: 13323057–13327587 (–)	2028	675	77,023.97	9.41	Plasma Membrane (4.667)
MiCNGC33	LOC123199977	Chr17: 659050–663360 (–)	2163	720	83,381.02	8.99	Plasma Membrane (4.360)
MiCNGC34	LOC123200530	Chr17: 10040631–10047558 (+)	2178	725	83,488.05	9.09	Plasma Membrane (4.053)
MiCNGC35	LOC123201033	Chr17: 11813705–11815638 (–)	696	231	26,664.04	9.05	Nuclear (1.519)
MiCNGC36	LOC123200218	Chr17: 11846751–11849774 (–)	690	229	26,194.33	8.47	Nuclear (1.544)
MiCNGC37	LOC123200982	Chr17: 12162919–12170581 (+)	2136	711	81,639.43	9.03	Plasma Membrane (4.349)
MiCNGC38	LOC123201393	Chr18: 10879862–10886175 (+)	2061	686	79,312.97	9.09	Plasma Membrane (4.272)
MiCNGC39	LOC123204873	Chr20: 2710625–2713311 (+)	2052	683	79,142.16	9	Plasma Membrane (4.212)
MiCNGC40	LOC123206450	NW_025401129.1: 250730–254202 (–)	2229	742	85,358.83	9.37	Plasma Membrane (3.988)
MiCNGC41	LOC123206532	NW_025401132.1: 147597–150404 (+)	2052	683	79,185.18	9.05	Plasma Membrane (4.213)
MiCNGC42	LOC123206927	NW_025401145.1: 36673–40482 (+)	2151	716	82,061.84	9.54	Plasma Membrane (4.714)
MiCNGC43	LOC123208231	NW_025401260.1: 224–2797 (–)	1176	391	44,867.26	9.23	Plasma Membrane (3.815)

2.2. Phylogenetic Relationships of Mango CNGC Genes

The CNGC proteins of *Arabidopsis*, rice, Amborella, sweet orange and mango were selected to construct the maximum-likelihood phylogenetic tree (Figure 2). Finally, four groups (I–IV) were generated, where almost the same quantities of CNGC proteins from the four species existed in each group. Interestingly, only sweet orange and mango CNGC proteins were clustered into group IV-C. Mango CNGC proteins were further aligned to identify their conserved domains. The results showed that most of them contained the CNBD domain ([L]-X(0,1,2)-[G]-X(1,3)-G-X(1,2)-[L]-[L]-X(0,1)-[W]-X(0,2)-[L]-X(0,7,8,9,10,18)-[P]-X-S-X(10)-[E]-A-[F]-X(0,1)-L) except *MiCNGC43* (Figure S2). However, nine mango CNGC proteins lost the N-termini due to evolution issues, namely *MiCNGC10*, *11*, *15*, *21*, *25*, *27*, *28*, *35* and *36*. We further calculated the values of synonymous substitutions (Ks), nonsynonymous site (Ka) and their ratio (Ka/Ks). The results indicated that all the Ka/Ks values were below 1 in homologous gene pairs (Table S2).

2.3. In Silico Expression of CNGC Genes in Mango Tissues

We further examined the expression levels of mango CNGC genes in leaf, fruit peel and fruit flesh based on published transcriptome data. The expression data were normalized into fragments per kilobase of exon model per million mapped fragments (FPKM) (Table S3). *MiCNGC17*, *19* and *22* were relatively expressed at high levels in all three tissues (FPKM > 10) (Figure 3). Several tissue-specific expressed mango CNGC genes were revealed too, such as *MiCNGC13*, *31* and *38* in leaf and *MiCNGC4*, *9*, *36* and *34* in fruit peel. At the same time, 10 mango CNGC genes displayed extremely low expression (FPKM < 10) in all three tissues, namely *MiCNGC2*, *11*, *14*, *24*, *30*, *33*, *35*, *37*, *42* and *43*, whereas 23 genes showed no expression detected by transcriptome sequencing (Table S3).

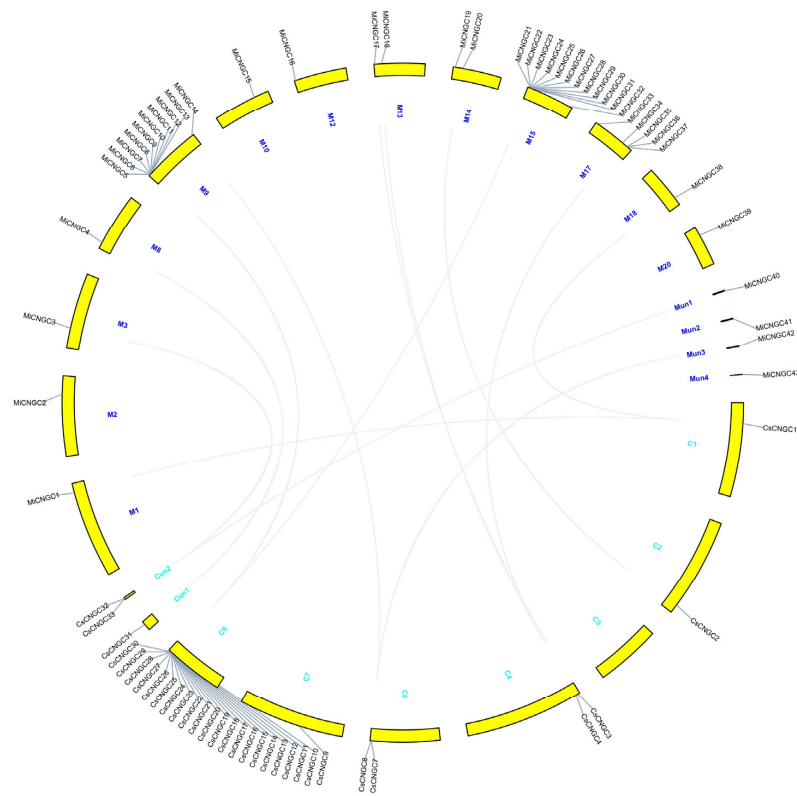


Figure 1. Chromosome distribution of CNGC genes in mango (blue) and sweet orange (light blue). The chromosome numbers are marked with numbers beside the chromosomes. Homologous gene pairs between the two species are linked with lines. The ‘un’ represents unanchored scaffolds.

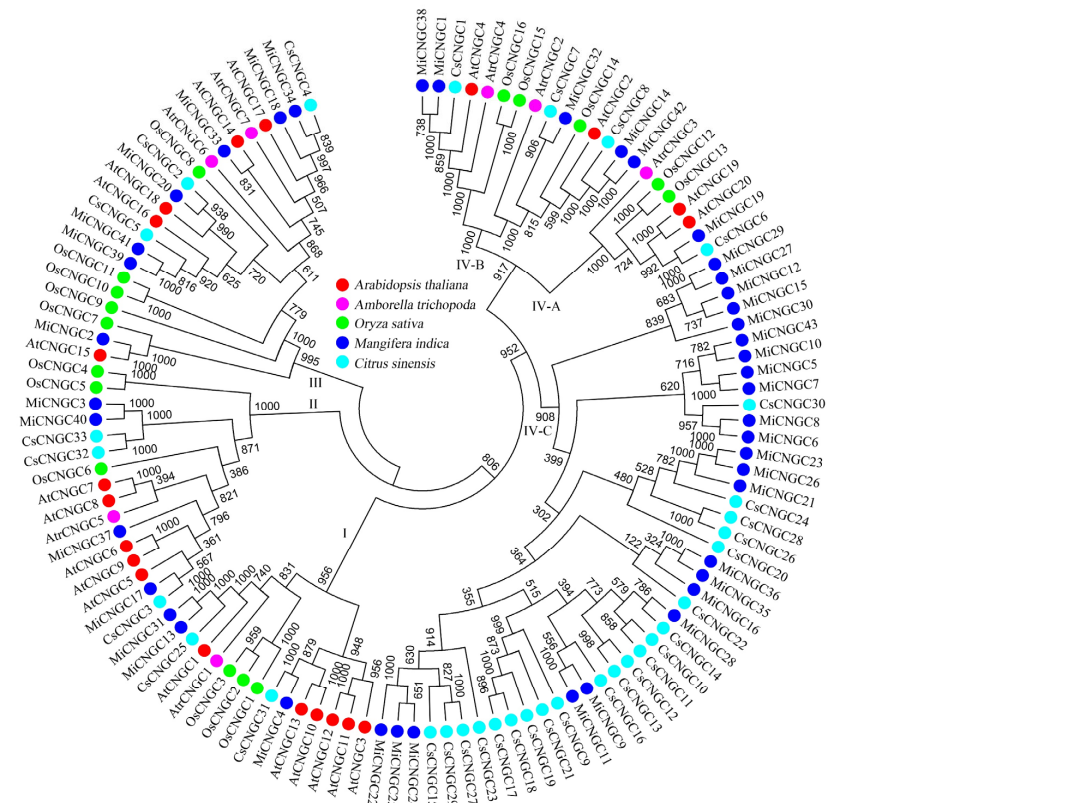


Figure 2. Maximum-likelihood phylogenetic tree of CNGC proteins in *Arabidopsis thaliana* (red), *Amborella trichopoda* (pink), *Oryza sativa* (green), *Mangifera indica* (blue) and *Citrus sinensis* (light blue).

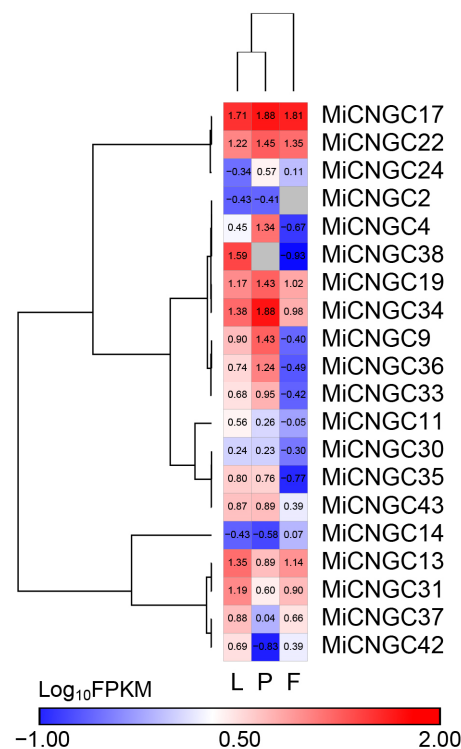


Figure 3. In silico expression of mango CNGC genes in different tissues, including leaf (L), fruit peel (P) and fruit flesh (F).

2.4. In Silico Expression of CNGC Genes under Cold Stress in Mango Fruit Peel

In order to evaluate their molecular functions under cold stress in fruit peel, moderate (12 °C) and extreme (5 °C) temperatures were chosen to compare CNGC expression patterns. The two treatments allow us to better understand the expression tendency of CNGC genes under cold stress. The results indicated that most CNGC genes (33 of 43) showed no or relatively low expression levels (FPKM < 10) under cold treatments of both 5 and 12 °C, implying that they might play minimal roles for cold tolerance (Table S3). However, 10 CNGC genes showed higher expression triggered by cold stress (Figure 4). Among these, three of them showed moderate expression patterns under 12 °C, but more than three-fold upregulated expression level under 5 °C (*MiCNGC4*, 9 and 34). Five genes showed similar expression patterns whether at 5 or 12 °C (*MiCNGC13*, 17, 19, 31 and 36), while *MiCNGC13* and 36 were up and downregulated over 3-fold under 5 °C after prolonged 14-day cold treatment, respectively. Moreover, *MiCNGC22* and *MiCNGC33* showed absolutely opposite expression patterns under the two degrees.

2.5. Expression Profiles of CNGC Genes under Cold Stress in Mango Leaf

To better understand how the CNGC genes affect cold stress response in mango plant, 10 mango CNGC genes were selected for qRT-PCR validation in mango leaf. These genes include five with expression changes over threefold under cold stress in fruit peel and five with FPKM values over 10 in leaf. The results indicated that most genes were upregulated after cold treatment in leaf except *MiCNGC4* (Figure 5). Among these, six were up-regulated more than threefold, namely *MiCNGC9*, 13, 17, 22, 31 and 38. Additionally, the expression of *MiCNGC13* was not significantly affected when temperature was higher than 4 °C, indicating that *MiCNGC13* might have leaf- and fruit-peel-specific temperature sensitivity.

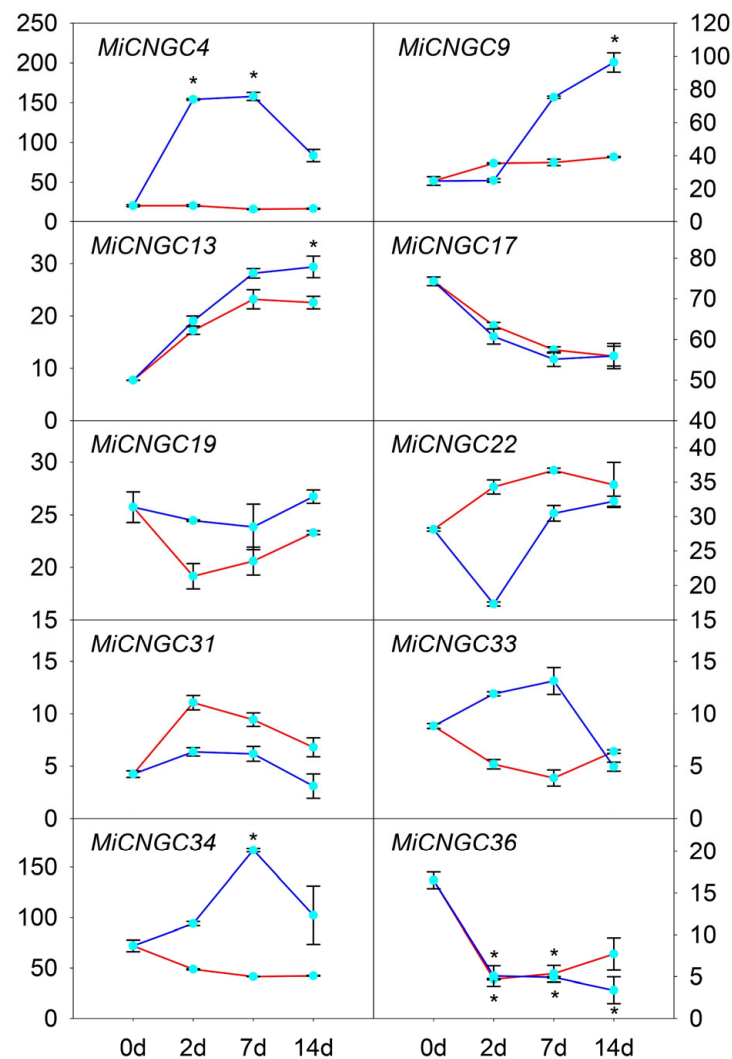


Figure 4. In silico expression of *CNGC* genes under cold stress of (blue) and 12 °C (red) in mango fruit peel. The x-axis represents the samples collected at 0, 2, 7 and 14 days after treatment. The y-axis represents FPKM values. The error bar represents the standard error. * represents that the expression level was up or downregulated over 3-fold.

2.6. Positively Correlated Mango *CNGC* Genes with MDA Contents

The content of malondialdehyde (MDA) is usually considered as a lipid peroxidation index that indicates the damage of stress. We therefore further measured MDA in mango leaf to evaluate the physiological effects of cold stress. As expected, MDA contents were significantly increased under cold treatment, specially under 2 °C (Figure 6A). This result suggested that temperatures under 2 °C might cause irreversible damage to the mango plant. To further determine whether *CNGC* genes regulate MDA level or not, we performed correlation analysis to explore *CNGC* genes that were highly correlated with MDA contents. The results showed that three and five *CNGC* genes were positively correlated with MDA contents with significant correlation coefficients at 0.05 ($R > 0.532$) and 0.01 ($R > 0.661$) cut-offs, respectively.

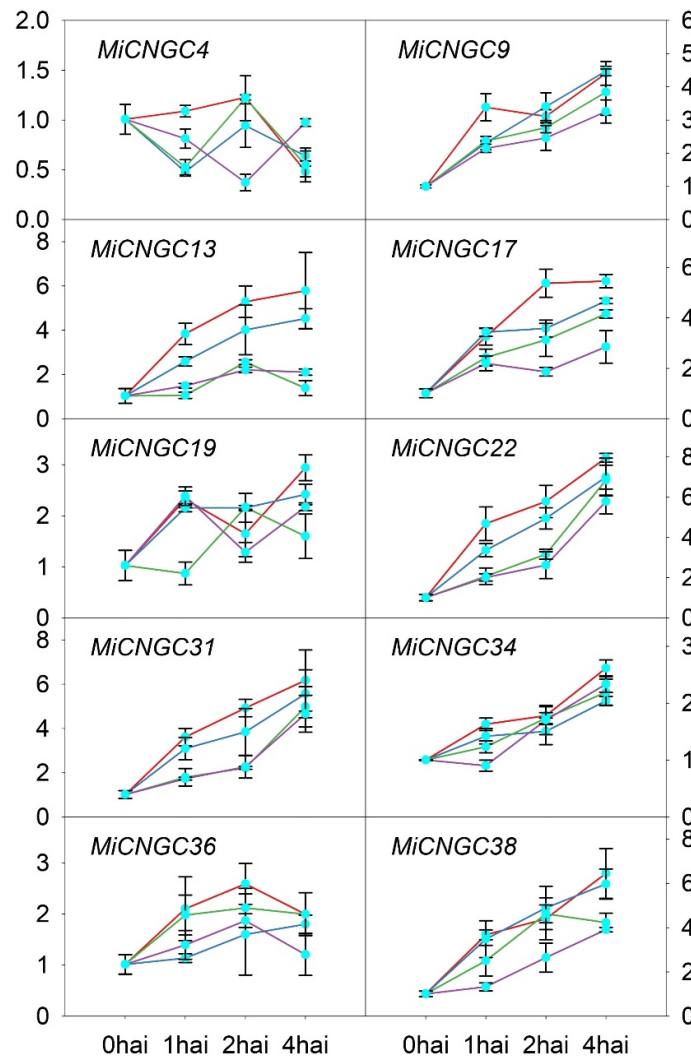


Figure 5. The expression of CNGC genes under cold stress of 2 (red), 4 (blue), 6 (green) and 8 °C (purple) in mango leaf according to qRT-PCR. The x-axis represents the samples collected at 0, 1, 2 and 4 h after incubation (hai) at different temperatures. The y-axis represents the values of $2^{-\Delta\Delta C_t}$. The error bar represents the standard error.

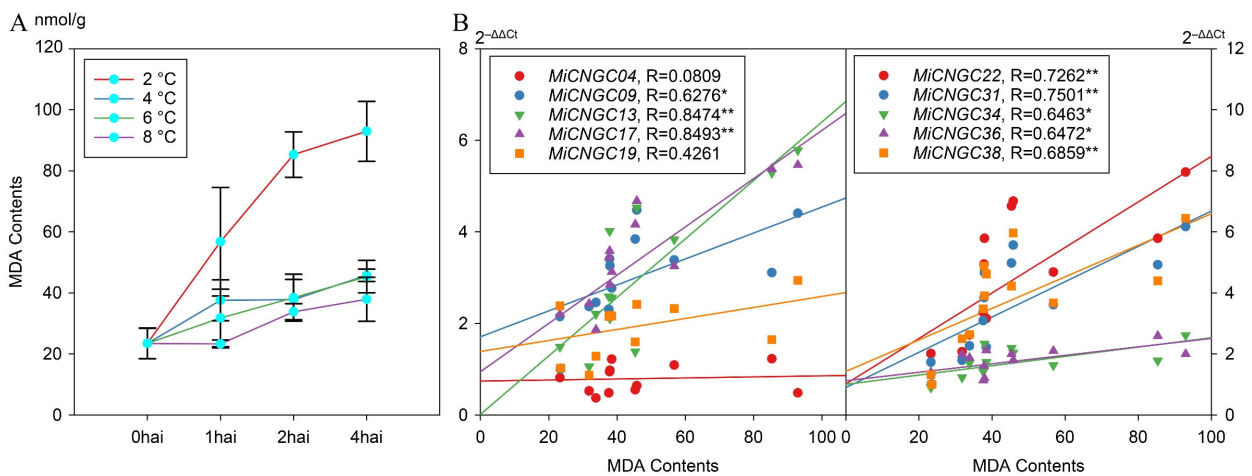


Figure 6. The MDA contents under cold stress of 2 (red), 4 (blue), 6 (green) and 8 °C (purple) in mango leaf (A) and their correlations with the relative expression levels of CNGC genes (B). * and ** represent that the correlation coefficients are significant at 0.05 ($R > 0.532$) and 0.01 ($R > 0.661$) levels, respectively.

3. Discussion

3.1. Species-Specific Expansion of CNGC Family in Mango

In the present study, we have successfully identified 7, 33 and 43 CNGC genes in Amborella, sweet orange and mango (Tables 1 and S1). As a basal angiosperm, Amborella has a relatively small number of CNGC genes compared with other four species (Figure 2). Beyond this, these genes are almost evenly distributed into three groups (I, II and III) and two subgroups (IV-A and IV-B), indicating the conserved evolution patterns and pressure among these groups [4]. Interestingly, there is a subgroup (IV-C) containing CNGC genes from either mango (23) or sweet orange (21). Most of them are distributed at chromosomes 9 and 15 in mango (18) and chromosome 9 in sweet orange (21) (Figure 1), verifying their Sapindales classification. However, the species-specific expansion of CNGC genes among mango and sweet orange also emphasizes the species divergence during evolution [32]. In addition, mango CNGC genes are classified into two major gene clusters, which might be divided from the same cluster during the hypothetical auto-diploidization [24]. Seven mango CNGC genes contain short coding regions (<1000 bp), such as *MiCNGC10*, *MiCNGC28* and so on (Table 1), which might be caused by frequent chromosomal recombination (Table S3) [33]. They might lose the function of Ca²⁺-permeable channels without complete transmembrane structure (Figure S1), which also affected their subcellular localizations predicted by CELLO.

3.2. Candidate CNGC Genes in Cold Stress Response in Mango

The in silico expression of CNGC genes in mango tissues illustrates that mango CNGC genes have tissue-specific expression patterns (Figure 3). The high and constitutive expression of *MiCNGC17* indicate that it might affect the whole mango development period. We further evaluated the expression of CNGC genes under cold stress to identify candidate regulators that contribute to cold tolerance. As shown, five *MiCNGCs* in fruit peel and five in leaf displayed more than three-fold upregulation of gene expression; specifically, *MiCNGC9* and *MiCNGC13* are induced in both tested tissues suggesting their potential functions under cold stress (Figures 4 and 5). Since MDA is the main indicator of cell membrane integrity [34], we observed that MDA content is significantly increased at 2 °C compared with 4, 6 and 8 °C (Figure 6A), which means that lower temperature leads higher damage. Then we revealed that eight *MiCNGCs* are positively correlated with MDA by correlation analysis (Figure 6B), emphasizing that *MiCNGCs* might regulate MDA content to adjust cell membrane integrity. Therefore, these eight genes could be considered as early cold-responsive markers in the mango leaf, among which *MiCNGC13* ranks first as the early cold-responsive maker gene in the mango leaf and fruit peel.

4. Materials and Methods

4.1. Bioinformatic Analysis of CNGC Genes

CNGC protein sequences of *Arabidopsis* and rice were selected as queries to search homologous proteins using the Blastp method [4,35]. The genomes of Amborella, sweet orange and mango were set as targets for sequence retrieval [24,30,31]. The details of CNGC genes in Amborella and sweet orange are listed in Table S1. The accession numbers and chromosome positions of mango CNGC genes are in Table 1 and were further used to illustrate their distribution in chromosomes using TBtools software [36]. The sequence features of length, molecular weight and pI were predicted using the ProtParam tool with subcellular localization predicted using CELLO software [37,38]. The TMHMM2.0 software was selected to predict the transmembrane helices in CNGC proteins [39]. A maximum-likelihood phylogenetic tree was constructed for phylogenetic analysis with bootstrap values of 1000 using MEGA 7.0 software [40]. The mango CNGC proteins were further aligned by DNAMAN7 software to examine the conserved domains [41]. The Ks, Ka and Ka/Ks values were calculated using TBtools software [36].

4.2. In Silico Gene Expression Analysis

The raw data of transcriptome sequencing were downloaded from the Sequence Read Archive (SRA) database [42]. The raw data of leaf (SRR3288569), fruit peel (SRR2960401) and fruit flesh (SRR11060165) were selected to evaluate the expression patterns of *CNGC* genes in different mango tissues. The raw data of cold-treated fruit peel (SRP066658) were selected to evaluate the expression patterns of *CNGC* genes in mango fruit peels under cold stress, which were generated at 0, 2, 7 and 14 days after storage at 5 and 12 °C [43]. All raw data were trimmed to generate clean reads, which were further mapped to mango *CNGC* genes to calculate FPKM values for each gene with the RSEM software [44,45]. The heat map was generated using Morpheus software [46]. The hierarchical clustering method was selected to cluster the FPKM values at the levels of tissues and genes [47].

4.3. Plant Materials and Treatment

The mango variety Hongyu was selected for cold treatment. Experiments were carried out in a mango garden (109.11° E, 19.22° N) at Jishi Village, Changjiang, China. The branches of 15-year-old trees were put into RR-CTC806C incubators (Rainroot Scientific, Beijing, China) for cold treatments at four temperatures, namely 2, 4, 6 and 8 °C. After that, leaves were collected at 0, 1, 2 and 4 h. Leaves from two branches were put together as one sample and each sample was repeated three times as a biological replicate. All the samples were stored at −80 °C before further analysis.

4.4. Quantitative PCR and MDA Assay

Total RNA was isolated from each sample using the Tiangen RNA prep Pure Plant Kit (Tiangen Biomart, Beijing, China) and then transcribed into cDNA using the GoScript Reverse Transcription System (Promega, Madison, WI, USA) [48]. Quantitative PCR was conducted with the QuantStudio 6 Flex Real-Time PCR System (Thermo Fisher Scientific, Waltham, MA, USA). The reaction program contained three stages of initiation (94 °C for 30 s), 40 cycles (94 °C for 5 s and 60 °C for 30 s) and dissociation. The TransStart Tip Green qPCR SuperMix (Transgen Biotech, Beijing, China) was selected as the reaction solution, containing 10 µL supermix, 0.4 µL Passive Reference Dye, 1 µL cDNA, 0.5 µL of two primers and 7.6 µL nuclease-free water. Each sample was repeated three times as technical replicates. The Primer 3 software was used for primer design, and *MiActin* was selected as a reference gene (Table 2) [49]. The relative expression levels were calculated with the $\Delta\Delta C_t$ method as previously described [50,51]. The MDA contents were examined using the Malondialdehyde (MDA) Content Assay Kit (Solarbio, Beijing, China) according to the manufacturer's instruction [52]. About 0.1 g of each sample was broken into powder in liquid nitrogen and isolated with 1 mL Extraction reagent, which was fully homogenized in ice and centrifuged for supernatant (8000× *g* for 10 min at 4 °C). A total of 100 µL supernatant was mixed with 300 µL MDA working reagent and 100 µL Reagent III. Distilled water was selected as a blank reference. The mixtures of samples (T) and distilled water (B) were incubated for 60 min under 100 °C, which were cooled and centrifuged (10,000× *g* for 10 min) for supernatant at room temperature. The supernatants of mixtures (200 µL) were placed in a 96-well flat-bottom plate for the detection of absorbance (A) at 450, 532 and 600 nm with the Biotek Synergy H1 system (Agilent Technologies, Lexington, MA, USA). The MDA content was calculated with the following formula, $MDA \text{ (nmol/g)} = (12.9 \times (\Delta A_{532} - \Delta A_{600}) - 1.12 \times \Delta A_{450}) \times V_{rv} \div (W \times V_s \div V_{sv}) = 5 \times (12.9 \times (\Delta A_{532} - \Delta A_{600}) - 1.12 \times \Delta A_{450}) \div W$. V_{rv} , V_s , V_{sv} and W represent total reaction volume (0.5 mL), sample volume (0.1 mL), the volume of Extraction reagent (1 mL) and sample weight, respectively. $\Delta A_{450} = A_{450}(T) - A_{450}(B)$, $\Delta A_{532} = A_{532}(T) - A_{532}(B)$, $\Delta A_{600} = A_{600}(T) - A_{600}(B)$.

Table 2. Primers used for qRT-PCR analysis.

Genes	Forward Primer	Reverse Primer	Product Size (bp)	Accession Number
<i>MiCNGC4</i>	TTTACTGCTTCTGGTGGGGT	AGGGAGCAAACGATGAGACA	236	XM_044646600.1
<i>MiCNGC9</i>	TCAGCTTCCTCGTTGACCTT	CTTCCCGCTTCCAACATCAG	226	XM_044649431.1
<i>MiCNGC13</i>	TCGGGCTTCAGGATTCTTGT	CCCAGTCCACCTCTTCATGT	196	XM_044650230.1
<i>MiCNGC17</i>	CTTCAAACGAGCACCTTCCC	TCTCGTGTTCCTCAACCACT	246	XM_044608894.1
<i>MiCNGC19</i>	ACTTGGGAATGTCAGGAGCA	CCAACAACATGACCAGCCAA	193	XM_044610397.1
<i>MiCNGC22</i>	TCACATGGGCTCTAGATGGC	AAACAGAGTCATCCGGCAGA	175	XM_044612662.1
<i>MiCNGC31</i>	GACTTGGGCAGCTTGTTC	TGAATCCTTGCCTTCCGAGT	216	XM_044612575.1
<i>MiCNGC34</i>	CGCCGTTTTGACCAGTACAA	AGCATCTCGGTTACAGGGTC	248	XM_044615727.1
<i>MiCNGC36</i>	GCAAGACAGAGCAGTGGATG	TCCTCTAATGCCGATTCCGCT	232	XM_044615370.1
<i>MiCNGC38</i>	ATTCTCCCTCTCCCTCAGGT	TGTGCCGAAAATGTAGCCAG	183	XM_044616876.1
<i>MiActin</i>	CCACTGCTGAACGGGAAAT	GTGATGGCTGGAAGAGGAC	192	HQ585999.1

5. Conclusions

Extreme cold weather is a significant threat to the tropical fruit tree mango. Thus, we carried out a genome-wide analysis and assessed the expression of mango *CNGC* genes under cold stress, due to their importance in calcium-mediated development and cold response. The result revealed 43 *CNGC* genes with species-specific expansion in the mango genome. In silico expression analysis indicated their tissue-specific expression patterns and five differentially expressed *CNGC* genes under cold stress in mango fruit peel. The results of the qRT-PCR validation and MDA assay revealed five differentially expressed *CNGC* genes under cold stress in the mango leaf, which are also positively correlated with MDA contents. These results indicate a candidate early cold-responsive marker gene, *MiCNGC13*, in the mango leaf and fruit peel, which will be helpful to future studies related to cold stress in mango.

Supplementary Materials: The following supporting information can be downloaded at: <https://www.mdpi.com/article/10.3390/plants12030592/s1>, Figure S1: Transmembrane topology analysis for mango *CNGC* proteins; Figure S2: Alignment of *CNGC* proteins in mango; Table S1: Details of *CNGC* genes in amborella and sweet orange; Table S2: The values of synonymous substitutions (Ks), nonsynonymous site (Ka) and their ratio (Ka/Ks) in homologous gene pairs.; Table S3: FPKM values of mango *CNGC* genes in different tissues and under cold stress.

Author Contributions: Conceptualization, Y.Z., J.Z. and X.H.; formal analysis, Y.Z., Y.L., and X.H.; investigation, Y.Z., Y.L., J.Y., X.Y., S.C., M.Z. and Y.H.; writing—original draft preparation, Y.Z. and X.H.; writing—review and editing, Z.X.; supervision, J.Z.; funding acquisition, J.Z. All authors have read and agreed to the published version of the manuscript.

Funding: This research was funded by National Key Research and Development Program of China [2019YFD1002203] and the innovation platform for Academicians of Hainan Province.

Data Availability Statement: All data are contained within the article or Supplementary Materials.

Conflicts of Interest: The authors declare no conflict of interest.

References

- Kaplan, B.; Sherman, T.; Fromm, H. Cyclic nucleotide-gated channels in plants. *FEBS Lett.* **2007**, *581*, 2237–2246. [[CrossRef](#)] [[PubMed](#)]
- Baloch, A.A.; Raza, A.M.; Rana, S.S.A.; Ullah, S.; Khan, S.; Zaib-Un-Nisa; Zahid, H.; Malghani, G.K.; Kakar, K.U. BrCNGC gene family in field mustard: Genome-wide identification, characterization, comparative synteny, evolution and expression profiling. *Sci. Rep.* **2021**, *11*, 24203. [[CrossRef](#)] [[PubMed](#)]
- Jha, S.K.; Sharma, M.; Pandey, G.K. Role of Cyclic Nucleotide Gated Channels in Stress Management in Plants. *Curr. Genom.* **2016**, *17*, 315–329. [[CrossRef](#)] [[PubMed](#)]
- Nawaz, Z.; Kakar, K.U.; Saand, M.A.; Shu, Q.Y. Cyclic nucleotide-gated ion channel gene family in rice, identification, characterization and experimental analysis of expression response to plant hormones, biotic and abiotic stresses. *BMC Genom.* **2014**, *15*, 853. [[CrossRef](#)] [[PubMed](#)]
- Saand, M.A.; Xu, Y.P.; Munyampundu, J.P.; Li, W.; Zhang, X.R.; Cai, X.Z. Phylogeny and evolution of plant cyclic nucleotide-gated ion channel (CNGC) gene family and functional analyses of tomato CNGCs. *DNA Res.* **2015**, *22*, 471–483. [[CrossRef](#)] [[PubMed](#)]

6. Zia, K.; Rao, M.J.; Sadaqat, M.; Azeem, F.; Fatima, K.; Tahir Ul Qamar, M.; Alshammari, A.; Alharbi, M. Pangenome-wide analysis of cyclic nucleotide-gated channel (CNGC) gene family in *Citrus* spp. Revealed their intraspecies diversity and potential roles in abiotic stress tolerance. *Front. Genet.* **2022**, *13*, 1034921. [[CrossRef](#)] [[PubMed](#)]
7. Zhao, J.; Peng, S.; Cui, H.; Li, P.; Li, T.; Liu, L.; Zhang, H.; Tian, Z.; Shang, H.; Xu, R. Dynamic Expression, Differential Regulation and Functional Diversity of the CNGC Family Genes in Cotton. *Int. J. Mol. Sci.* **2022**, *23*, 2041. [[CrossRef](#)]
8. Demidchik, V.; Shabala, S.; Isayenkov, S.; Cuin, T.A.; Pottosin, I. Calcium transport across plant membranes: Mechanisms and functions. *New Phytol.* **2018**, *220*, 49–69. [[CrossRef](#)]
9. Gobert, A.; Park, G.; Amtmann, A.; Sanders, D.; Maathuis, F.J. Arabidopsis thaliana cyclic nucleotide gated channel 3 forms a non-selective ion transporter involved in germination and cation transport. *J. Exp. Bot.* **2006**, *57*, 791–800. [[CrossRef](#)]
10. Gu, L.L.; Gao, Q.F.; Wang, Y.F. Cyclic nucleotide-gated channel 18 functions as an essential Ca²⁺ channel for pollen germination and pollen tube growth in Arabidopsis. *Plant Signal. Behav.* **2017**, *12*, e1197999. [[CrossRef](#)]
11. Ma, W.; Smigel, A.; Walker, R.K.; Moeder, W.; Yoshioka, K.; Berkowitz, G.A. Leaf senescence signaling: The Ca²⁺-conducting Arabidopsis cyclic nucleotide gated channel2 acts through nitric oxide to repress senescence programming. *Plant Physiol.* **2010**, *154*, 733–743. [[CrossRef](#)] [[PubMed](#)]
12. Shih, H.W.; DePew, C.L.; Miller, N.D.; Monshausen, G.B. The Cyclic Nucleotide-Gated Channel CNGC14 Regulates Root Gravitropism in *Arabidopsis thaliana*. *Curr. Biol.* **2015**, *25*, 3119–3125. [[CrossRef](#)] [[PubMed](#)]
13. Tan, Y.Q.; Yang, Y.; Zhang, A.; Fei, C.F.; Gu, L.L.; Sun, S.J.; Xu, W.; Wang, L.; Liu, H.; Wang, Y.F. Three CNGC Family Members, CNGC5, CNGC6, and CNGC9, Are Required for Constitutive Growth of Arabidopsis Root Hairs as Ca²⁺-Permeable Channels. *Plant Commun.* **2019**, *1*, 100001. [[CrossRef](#)] [[PubMed](#)]
14. Tunc-Ozdemir, M.; Rato, C.; Brown, E.; Rogers, S.; Mooneyham, A.; Frietsch, S.; Myers, C.T.; Poulsen, L.R.; Malhó, R.; Harper, J.F. Cyclic nucleotide gated channels 7 and 8 are essential for male reproductive fertility. *PLoS ONE* **2013**, *8*, e55277. [[CrossRef](#)]
15. Tunc-Ozdemir, M.; Tang, C.; Ishka, M.R.; Brown, E.; Groves, N.R.; Myers, C.T.; Rato, C.; Poulsen, L.R.; McDowell, S.; Miller, G.; et al. A cyclic nucleotide-gated channel (CNGC16) in pollen is critical for stress tolerance in pollen reproductive development. *Plant Physiol.* **2013**, *161*, 1010–1020. [[CrossRef](#)]
16. Chin, K.; DeFalco, T.A.; Moeder, W.; Yoshioka, K. The Arabidopsis cyclic nucleotide-gated ion channels AtCNGC2 and AtCNGC4 work in the same signaling pathway to regulate pathogen defense and floral transition. *Plant Physiol.* **2013**, *163*, 611–624. [[CrossRef](#)]
17. Guo, K.M.; Babourina, O.; Christopher, D.A.; Borsics, T.; Rengel, Z. The cyclic nucleotide-gated channel, AtCNGC10, influences salt tolerance in Arabidopsis. *Physiol. Plant.* **2008**, *134*, 499–507. [[CrossRef](#)]
18. Niu, W.T.; Han, X.W.; Wei, S.S.; Shang, Z.L.; Wang, J.; Yang, D.W.; Fan, X.; Gao, F.; Zheng, S.Z.; Bai, J.T.; et al. Arabidopsis cyclic nucleotide-gated channel 6 is negatively modulated by multiple calmodulin isoforms during heat shock. *J. Exp. Bot.* **2020**, *71*, 90–104. [[CrossRef](#)]
19. Oranab, S.; Ghaffar, A.; Kiran, S.; Yameen, M.; Munir, B.; Zulfiqar, S.; Abbas, S.; Batool, F.; Farooq, M.U.; Ahmad, B.; et al. Molecular characterization and expression of cyclic nucleotide gated ion channels 19 and 20 in *Arabidopsis thaliana* for their potential role in salt stress. *Saudi J. Biol. Sci.* **2021**, *28*, 5800–5807. [[CrossRef](#)]
20. Sunkar, R.; Kaplan, B.; Bouché, N.; Arazi, T.; Dolev, D.; Talke, I.N.; Maathuis, F.J.; Sanders, D.; Bouchez, D.; Fromm, H. Expression of a truncated tobacco NtCBP4 channel in transgenic plants and disruption of the homologous Arabidopsis CNGC1 gene confer Pb²⁺ tolerance. *Plant J.* **2000**, *24*, 533–542. [[CrossRef](#)]
21. Yoshioka, K.; Moeder, W.; Kang, H.G.; Kachroo, P.; Masmoudi, K.; Berkowitz, G.; Klessig, D.F. The chimeric Arabidopsis CYCLIC NUCLEOTIDE-GATED ION CHANNEL11/12 activates multiple pathogen resistance responses. *Plant Cell* **2006**, *18*, 747–763. [[CrossRef](#)] [[PubMed](#)]
22. Upadhyay, S.K. Calcium Channels, OST1 and Stomatal Defence: Current Status and Beyond. *Cells* **2023**, *12*, 127. [[CrossRef](#)] [[PubMed](#)]
23. Tharanathan, R.N.; Yashoda, H.M.; Prabha, T.N. Mango (*Mangifera indica* L.), “the king of fruits”—An overview. *Food Rev. Int.* **2006**, *22*, 29. [[CrossRef](#)]
24. Wang, P.; Luo, Y.; Huang, J.; Gao, S.; Zhu, G.; Dang, Z.; Gai, J.; Yang, M.; Zhu, M.; Zhang, H.; et al. The genome evolution and domestication of tropical fruit mango. *Genome Biol.* **2020**, *21*, 60. [[CrossRef](#)]
25. Sherman, A.; Rubinstein, M.; Eshed, R.; Benita, M.; Ish-Shalom, M.; Sharabi-Schwager, M.; Rozen, A.; Saada, D.; Cohen, Y.; Ophir, R. Mango (*Mangifera indica* L.) germplasm diversity based on single nucleotide polymorphisms derived from the transcriptome. *BMC Plant Biol.* **2015**, *15*, 277. [[CrossRef](#)]
26. Sun, C.; Lin, W.; Huang, C.; Wu, L.; Chen, J.; Wang, J.; Lin, H. GIS-based Risk Zoning and Assessment of Mongo Cold and Freezing Injury in South China. *Chin. J. Agrometeorol.* **2022**, *43*, 563–575.
27. Lesk, C.; Rowhani, P.; Ramankutty, N. Influence of extreme weather disasters on global crop production. *Nature* **2016**, *529*, 84–87. [[CrossRef](#)]
28. Sanches, A.G.; Da Silva, M.B.; Fernandes, T.F.S.; Pedrosa, V.M.D.; Wong, M.C.C.; Gratao, P.L.; Teixeira, G.H.A. Reducing chilling injury in ‘Palmer’ mangoes submitted to quarantine cold treatment. *J. Sci. Food Agric.* **2022**, *102*, 6112–6122. [[CrossRef](#)]
29. Cui, Y.; Lu, S.; Li, Z.; Cheng, J.; Hu, P.; Zhu, T.; Wang, X.; Jin, M.; Wang, X.; Li, L.; et al. CYCLIC NUCLEOTIDE-GATED ION CHANNELS 14 and 16 Promote Tolerance to Heat and Chilling in Rice. *Plant Physiol.* **2020**, *183*, 1794–1808. [[CrossRef](#)]
30. Amborella Genome Project. The Amborella genome and the evolution of flowering plants. *Science* **2013**, *342*, 1241089. [[CrossRef](#)]
31. Xu, Q.; Chen, L.L.; Ruan, X.; Chen, D.; Zhu, A.; Chen, C.; Bertrand, D.; Jiao, W.B.; Hao, B.H.; Lyon, M.P.; et al. The draft genome of sweet orange (*Citrus sinensis*). *Nat. Genet.* **2013**, *45*, 59–66. [[CrossRef](#)] [[PubMed](#)]

32. Li, W.; Liu, W.; Wei, H.; He, Q.; Chen, J.; Zhang, B.; Zhu, S. Species-specific expansion and molecular evolution of the 3-hydroxy-3-methylglutaryl coenzyme A reductase (HMGR) gene family in plants. *PLoS ONE* **2014**, *9*, e94172. [[CrossRef](#)] [[PubMed](#)]
33. Hunter, N. Meiotic Recombination: The Essence of Heredity. *Cold Spring Harb. Perspect. Biol.* **2015**, *7*, a016618. [[CrossRef](#)] [[PubMed](#)]
34. Guo, X.; Liu, D.; Chong, K. Cold signaling in plants: Insights into mechanisms and regulation. *J. Integr. Plant Biol.* **2018**, *60*, 745–756. [[CrossRef](#)]
35. Altschul, S.F.; Gish, W.; Miller, W.; Myers, E.W.; Lipman, D.J. Basic local alignment search tool. *J. Mol. Biol.* **1990**, *215*, 403–410. [[CrossRef](#)]
36. Chen, C.; Chen, H.; Zhang, Y.; Thomas, H.R.; Frank, M.H.; He, Y.; Xia, R. TBtools—An Integrative Toolkit Developed for Interactive Analyses of Big Biological Data. *Mol. Plant* **2020**, *13*, 1194–1202. [[CrossRef](#)] [[PubMed](#)]
37. ProtParam Tool. Available online: web.expasy.org/protparam/ (accessed on 7 November 2022).
38. Yu, C.S.; Chen, Y.C.; Lu, C.H.; Hwang, J.K. Prediction of protein subcellular localization. *Proteins* **2006**, *64*, 643–651. [[CrossRef](#)] [[PubMed](#)]
39. Krogh, A.; Larsson, B.; Von Heijne, G.; Sonnhammer, E.L. Predicting transmembrane protein topology with a hidden Markov model: Application to complete genomes. *J. Mol. Biol.* **2001**, *305*, 567–580. [[CrossRef](#)]
40. Kumar, S.; Stecher, G.; Tamura, K. MEGA7: Molecular Evolutionary Genetics Analysis Version 7.0 for Bigger Datasets. *Mol. Biol. Evol.* **2016**, *33*, 1870–1874. [[CrossRef](#)]
41. DNAMAN—Bioinformatics Solutions. Available online: www.lynnon.com (accessed on 7 November 2022).
42. Sequence Read Archive. Available online: www.ncbi.nlm.nih.gov/sra (accessed on 7 November 2022).
43. Sivankalyani, V.; Sela, N.; Feygenberg, O.; Zemach, H.; Maurer, D.; Alkan, N. Transcriptome Dynamics in Mango Fruit Peel Reveals Mechanisms of Chilling Stress. *Front. Plant Sci.* **2016**, *7*, 1579. [[CrossRef](#)]
44. Li, B.; Dewey, C.N. RSEM: Accurate transcript quantification from RNA-Seq data with or without a reference genome. *BMC Bioinform.* **2011**, *12*, 323. [[CrossRef](#)] [[PubMed](#)]
45. Sharma, H.; Sharma, A.; Rajput, R.; Sidhu, S.; Dhillon, H.; Verma, P.C.; Pandey, A.; Upadhyay, S.K. Molecular Characterization, Evolutionary Analysis, and Expression Profiling of BOR Genes in Important Cereals. *Plants* **2022**, *11*, 911. [[CrossRef](#)] [[PubMed](#)]
46. Morpheus. Available online: software.broadinstitute.org/morpheus/ (accessed on 7 November 2022).
47. Zolfaghari, F.; Khosravi, H.; Shahriyari, A.; Jabbari, M.; Abolhasani, A. Hierarchical cluster analysis to identify the homogeneous desertification management units. *PLoS ONE* **2019**, *14*, e0226355. [[CrossRef](#)] [[PubMed](#)]
48. Huang, X.; Xiao, M.; Xi, J.; He, C.; Zheng, J.; Chen, H.; Gao, J.; Zhang, S.; Wu, W.; Liang, Y.; et al. De novo transcriptome assembly of Agave H11648 by Illumina sequencing and identification of cellulose synthase genes in Agave species. *Genes* **2019**, *10*, 103. [[CrossRef](#)] [[PubMed](#)]
49. Liu, F.; Wu, J.B.; Zhan, R.L.; Ou, X.C. Transcription Profiling Analysis of Mango-*Fusarium mangiferae* Interaction. *Front. Microbiol.* **2016**, *7*, 1443. [[CrossRef](#)] [[PubMed](#)]
50. Huang, X.; Wang, B.; Xi, J.; Zhang, Y.; He, C.; Zheng, J.; Gao, J.; Chen, H.; Zhang, S.; Wu, W.; et al. Transcriptome comparison reveals distinct selection patterns in domesticated and wild Agave species, the important CAM plants. *Int. J. Genom.* **2018**, *2018*, 5716518. [[CrossRef](#)]
51. Livak, K.J.; Schmittgen, T.D. Analysis of relative gene expression data using real-time quantitative PCR and the $2^{-\Delta\Delta C(T)}$ Method. *Methods* **2001**, *25*, 402–408. [[CrossRef](#)]
52. Sun, G.; Geng, S.; Zhang, H.; Jia, M.; Wang, Z.; Deng, Z.; Tao, S.; Liao, R.; Wang, F.; Kong, X.; et al. Matrilineal empowers wheat pollen with haploid induction potency by triggering postmitosis reactive oxygen species activity. *New Phytol.* **2022**, *233*, 2405–2414. [[CrossRef](#)]

Disclaimer/Publisher’s Note: The statements, opinions and data contained in all publications are solely those of the individual author(s) and contributor(s) and not of MDPI and/or the editor(s). MDPI and/or the editor(s) disclaim responsibility for any injury to people or property resulting from any ideas, methods, instructions or products referred to in the content.